A conserved CCCH-type zinc finger protein regulates mRNA nuclear adenylation and export

Jessica A. Hurt,[1] Robert A. Obar,[2] Bo Zhai,[2] Natalie G. Farny,[1] Steven P. Gygi,[2] and Pamela A. Silver[1]

[1]Department of Systems Biology and [2]Department of Cell Biology, Harvard Medical School, Boston, MA 02115

Coupling of messenger RNA (mRNA) nuclear export with prior processing steps aids in the fidelity and efficiency of mRNA transport to the cytoplasm. In this study, we show that the processes of export and polyadenylation are coupled via the *Drosophila melanogaster* CCCH-type zinc finger protein CG6694/dZC3H3 through both physical and functional interactions. We show that depletion of dZC3H3 from S2R+ cells results in transcript hyperadenylation. Using targeted coimmunoprecipitation and liquid chromatography mass spectrometry (MS)/MS techniques, we characterize interactions of known components of the mRNA nuclear export and polyadenylation machineries with dZC3H3. Furthermore, we demonstrate the functional conservation of this factor, as depletion of its human homologue ZC3H3 by small interfering RNA results in an mRNA export defect in human cells as well. Nuclear polyadenylated (poly(A)) RNA in ZC3H3-depleted cells is sequestered in foci removed from SC35-containing speckles, indicating a shift from the normal subnuclear distribution of poly(A) RNA. Our data suggest a model wherein ZC3H3 interfaces between the polyadenylation machinery, newly poly(A) mRNAs, and factors for transcript export.

Introduction

Eukaryotic gene expression requires mRNAs to be transported from their site of transcription in the nucleus to their site of translation in the cytoplasm. As translation of improperly processed mRNAs is likely to be detrimental to a cell, the passage of mRNA molecules between these two compartments is highly regulated. Studies in yeast and higher eukaryotes have identified many conserved factors that are critical to proper mRNA processing, including transcription, 5′ capping, 3′ processing, splicing, and surveillance factors, to additionally be required for transcript nuclear export (Sommer and Nehrbass, 2005; Hagiwara and Nojima, 2007; Luna et al., 2008; for reviews see Reed and Cheng, 2005; Saguez et al., 2005). By physical and functional coupling of the export process to components of prior mRNA processing steps, the cell may impose checkpoints that must be satisfied before transcripts can be released into the cytoplasm.

Heterodimers of the essential export factors NXF1 (human Tap/yeast Mex67p) and p15 (human NXT1/yeast Mtr2p) mediate the export of most mRNAs by interfacing with components of the nuclear pore complex. However, the majority of cellular mRNAs interact inefficiently with NXF1/p15 heterodimers. Instead, they require adaptor proteins such as REF (RNA export factor; human Aly/yeast Yra1p) or SR (serine/arginine-rich) proteins to interact with these factors (Santos-Rosa et al., 1998; Huang et al., 2003). Although deposition of some adaptors occurs cotranscriptionally in yeast, these factors are recruited to the mRNA at a later stage in the splicing process in higher eukaryotes (for review see Reed and Cheng, 2005). Interactions of Aly and SR proteins with mRNAs are also likely to be stabilized by contacts with the exon junction complex. As exon junction complexes are deposited on mRNAs during the splicing process, they and their associated factors are well positioned to recruit export factors NXF1/p15 to fully spliced transcripts (Masuda et al., 2005; Cheng et al., 2006).

Substantial evidence indicates that the 3′ end processing of mRNAs is coupled to their export as well. Although the presence of proper 3′ cleavage signals can stimulate nuclear export of mRNAs (Eckner et al., 1991), mutations in cis in the 3′ processing signal sequences result in defective mRNA nuclear

Correspondence to Pamela A. Silver: pamela_silver@hms.harvard.edu

Abbreviations used in this paper: clp, clipper; CPSF, cleavage and polyadenylation specificity factor; dsRNA, double-stranded RNA; IP, immunoprecipitation; mRNP, messenger RNP particle; MS, mass spectrometry; PAP, poly(A) polymerase; poly(A), polyadenylated; swm, second mitotic wave missing; TAP, tandem affinity purification.

The Rockefeller University Press $30.00
J. Cell Biol. Vol. 185 No. 2 265–277
www.jcb.org/cgi/doi/10.1083/jcb.200811072

export in yeast and mammalian cells (Long et al., 1995; Custodio et al., 1999; Hammell et al., 2002). Defects in yeast 3′ processing factors cause transcript nuclear retention, sometimes specifically at sites of transcription (Brodsky and Silver, 2000; Hilleren et al., 2001; Hammell et al., 2002). In particular, the yeast factor Nab2p is implicated in both controlling polyadenylated (poly(A)) tail length as well as targeting transcripts to the nuclear periphery for export (Hector et al., 2002; Fasken et al., 2008). Interestingly, nuclear export requires the active process of polyadenylation, not only the presence of a poly(A) tail, to proceed (Huang and Carmichael, 1996). Together, these results suggest that the polyadenylation process actively recruits and positions factors properly onto transcripts that are necessary for their export. However, the identities of these factors and the mechanistic details of their recruitment, particularly in metazoan cells, are currently not well understood.

mRNA polyadenylation occurs via a two-step mechanism; first, an endonucleolytic cleavage of the nascent mRNA followed by the addition of a poly(A) tail to the upstream 3′ hydroxyl group (for review see Mandel et al., 2008). In mammals, the cleavage and polyadenylation specificity factor (CPSF) is required for both the cleavage event and the subsequent polyadenylation process. In this second step, CPSF acts in concert with nuclear poly(A) binding protein (fly PABP2 [poly(A) binding protein II]/human PABPN1) to tether poly(A) polymerase (PAP), which has low RNA-binding affinity itself, to the elongating 3′ tail and to stimulate processive polyadenylation (Bienroth et al., 1993; Kerwitz et al., 2003). As the reaction progresses, PABP2/PABPN1 molecules successively bind the adenylate residues, thus coating the tail and maintaining contacts with the extending PAP (Wahle, 1995). However, after addition of ∼200–300 adenine residues (the typical length of a mammalian mRNA tail; Brawerman, 1981), interactions between CPSF and PAP are likely no longer favorable and, via an ill-defined mechanism, the quaternary complex of CPSF, PABP2/PABPN1, PAP, and RNA is thought to disassemble.

Nuclear speckles, also known as interchromatin granule clusters or splicing speckles, are one of many nuclear subcompartments thought to aid in the progression of DNA and RNA processing events (Hall et al., 2006; Handwerger and Gall, 2006; Bernardi and Pandolfi, 2007; for review see Lamond and Spector, 2003). Speckles are devoid of chromatin but rich in numerous factors important to different stages of mRNA biogenesis such as small nuclear RNP particles, splicing factors, RNA polymerase II, and 3′ end processing factors, including CPSF and PABPN1 (Mintz et al., 1999; Saitoh et al., 2004). Poly(A) RNA species, including mRNAs as well as noncoding RNAs, are also specifically enriched within these domains (Carter et al., 1991; Xing et al., 1995; Johnson et al., 2000; Hutchinson et al., 2007; for review see Lamond and Spector, 2003). Thus, nuclear speckles are currently regarded as dynamic repositories of factors required for the proper splicing and processing of transcripts. Although specific messages have been localized both peripheral and internal to speckles (Xing et al., 1995; Johnson et al., 2000), questions still remain regarding the exact function of the speckle in transcript processing and the spatial relationship of messages to these domains during export.

Drosophila melanogaster factor CG6694 was identified in a genome-wide screen as required for the nuclear export of mRNAs (Farny et al., 2008). Harboring three CCCH-type zinc fingers near its C terminus, CG6694 possesses 27% sequence identity and 41% similarity to the 30-kD subunit of the *Drosophila* CPSF. The closest homologue of CG6694 in mouse, Zc3h3, was originally identified in a yeast two-hybrid study as a nuclear Smad-interacting protein (and thus termed Smicl [Smad-interacting CPSF-like factor]). Zc3h3 was additionally found to associate with subunits of CPSF and to have the ability to potentiate a Smad-dependent transcriptional event when proper 3′ end signal sequences were present in the responsive locus (Collart et al., 2005a). Later work further identified the *Xenopus laevis* homologue to be required for proper embryonic development also in a Smad-dependent manner (Collart et al., 2005b).

To investigate the coupling mechanisms that exist between the mRNA 3′ end processing and export machineries, we further explored the role that CG6694 has in these two processes. In this study, we demonstrate CG6694's importance in the proper polyadenylation and export of mRNAs in *Drosophila*. Through biochemical and genetic approaches, we demonstrate interactions of CG6694 with the export and polyadenylation machinery. We also illustrate its importance in mRNA processing in human cells, as depletion of its human homologue, ZC3H3, results in the aberrant accumulation of transcripts peripheral to nuclear speckles. Our data suggest that CG6694/ZC3H3 is a conserved modulator of mRNA processing after initiation of polyadenylation and before nuclear export.

Results

The C terminus of *Drosophila* CG6694/dZC3H3 is required for mRNA nuclear export

As part of a genome-wide RNAi screen, we identified nuclear *Drosophila* factor CG6694 as required for proper nuclear export of poly(A) RNA as well as of the endogenous heat shock protein mRNAs *HSP83* and *HSP70* from the nucleus of S2R+ cells (Farny et al., 2008). Fig. 1 A illustrates the nuclear accumulation of poly(A) RNA as indicated by a Cy3-labeled oligomer-dT(30) probe (Cy3-OdT), which is resultant upon double-stranded RNA (dsRNA)–mediated depletion of CG6694 from *Drosophila* S2R+ cells as compared with the steady-state cytoplasmic localization characteristic of control cells (depleted using GFP-targeting dsRNAs). Similarly, hybridization with gene-specific probes targeting the intronless *HSP70* and intron-containing *HSP83* messages revealed significant nuclear accumulation of both transcripts upon CG6694 depletion, indicating the role of this factor in their export as well. Given CG6694's homology to the human protein ZC3H3 (15% identity and 23% similarity), we will hereafter refer to this factor as dZC3H3.

dZC3H3 encodes a 597-aa protein that contains three CCCH-type zinc fingers near its C terminus and an N-terminal domain harboring no known functional homology (Fig. 1 B). In the C terminus, dZC3H3 possesses 27% sequence identity and 41% similarity to the 30-kD subunit of the 3′ processing complex CPSF, also known as clipper (clp). As *Drosophila* clp and

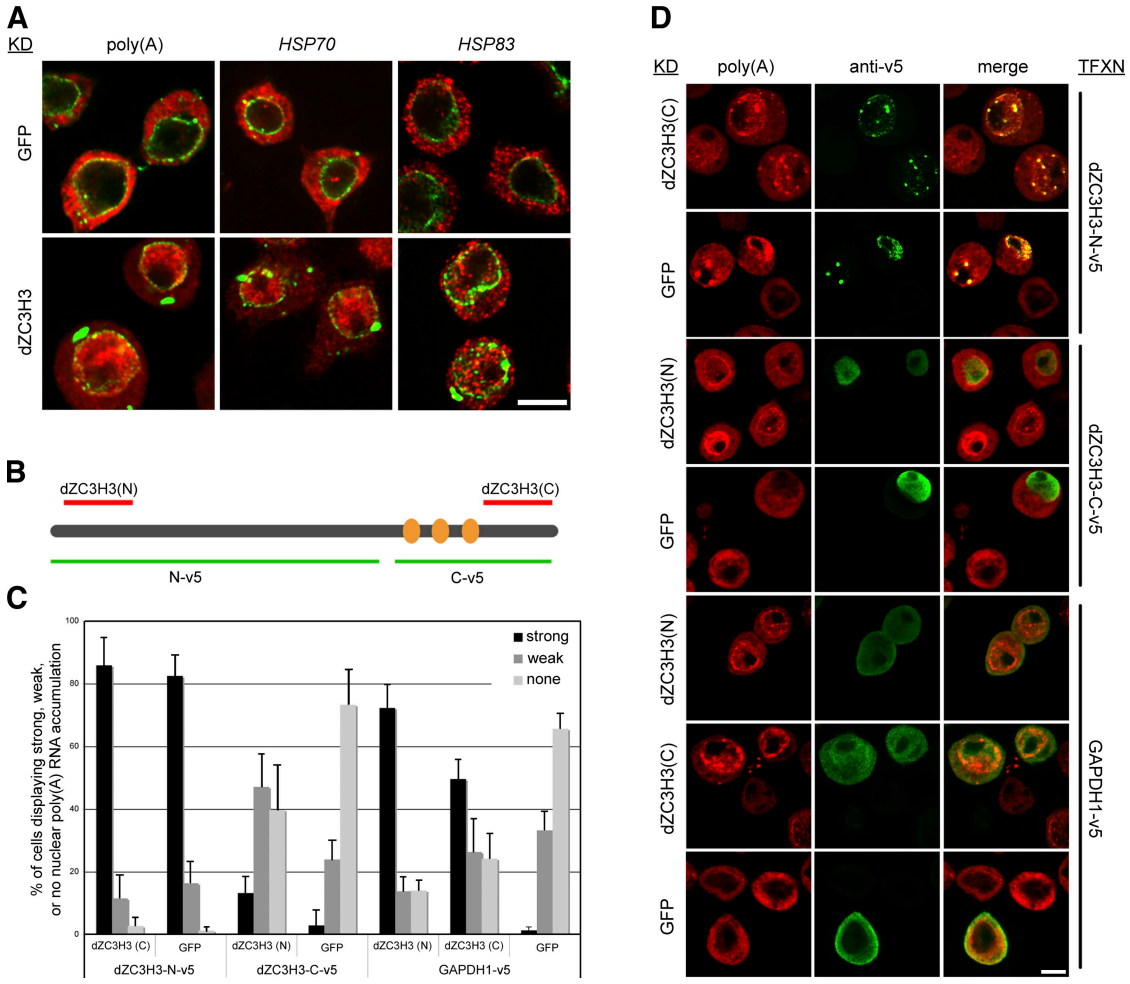

Figure 1. **dZC3H3 is required for nuclear export of bulk poly(A) RNA and specific messages.** (A) S2R+ cells depleted of dZC3H3 (bottom) or GFP (top) were fixed, permeabilized, and analyzed for RNA subcellular localization using Alexa Fluor 488–conjugated wheat germ agglutinin (green) to mark the nuclear rim and either a Cy3-OdT probe (left), *HSP70*-specific probes (middle), or an *HSP83*-specific probe (right; red). (B) Schematic of the dZC3H3 protein, its zinc finger domains (orange), composition of the v5-tagged deletion mutants (green), and sequences targeted by dsRNAs (red). (C) Overexpression of the C terminus of dZC3H3 (C-v5) partially rescues the poly(A) RNA nuclear export defect, whereas expression of the N terminus (N-v5) exacerbates the accumulation phenotype. The bar graph indicates the fraction of transfected cells displaying strong, weak, or no nuclear poly(A) RNA accumulation upon depletion of endogenous dZC3H3 or GFP and overexpression of various deletion mutants or GAPDH1-v5. (D) Representative images scored in C of S2R+ cells processed for poly(A) RNA localization (red) and immunofluorescence (v5; green) after being both depleted of endogenous dZC3H3 or GFP (labeled at left) and transfected with various v5-tagged deletion mutants (TFXN; labeled at right). Error bars indicate SDs of results between three experimental replicates. Bars, 5 µm.

mouse Smicl have both been shown to possess single-stranded DNA–binding activity and nuclease activity via their CCCH zinc fingers (Bai and Tolias, 1996; Collart et al., 2005a), we investigated whether this domain was sufficient to mediate dZC3H3's mRNA export function.

By assessing the ability of different regions of dZC3H3 to rescue the RNA export defect in dZC3H3 knockdown cells, we identified the C-terminal region of this factor to be required and partially sufficient to mediate poly(A) RNA nuclear export. *Drosophila* S2R+ cells were simultaneously depleted of endogenous dZC3H3 using one of two dsRNAs (dZC3H3(N) and dZC3H3(C)) and transfected with a v5-tagged dZC3H3 deletion mutant or GAPDH1 (Fig. 1 B). After fixation and processing for both poly(A) RNA and v5-tagged protein localization, populations of cells were assessed for the fraction of those transfected that yielded nuclear localized poly(A) RNA. Quantification and representative confocal fluorescence images of this experiment are given in Fig. 1 (C and D). Importantly, unlike some other RNA-binding proteins, full-length dZC3H3-v5 does not induce an export defect when overexpressed (Fig. S1; Windgassen and Krebber, 2003; Tavanez et al., 2005). However, cells transfected with GAPDH1-v5 and treated with either dZC3H3(C) or dZC3H3(N) harbor an abnormal level of nuclear poly(A) RNA (72% strong nuclear accumulation and 14% partial accumulation vs. 50% strong and 26% partial, respectively) as compared with cells treated with GFP dsRNAs (1% strong and 33% partial; Fig. 1, C and D [rows 5–7]). In contrast, cells transfected with the C terminus of dZC3H3 (dZC3H3-C–v5) and treated with dZC3H3(N) exhibit a reduced level of nuclear poly(A) RNA accumulation (13% strong; Fig. 1, C and D [row 3]). Thus, expression of dZC3H3-C–v5 partially restores the cytoplasmic localization of poly(A) RNA in cells that are depleted of endogenous dZC3H3.

Interestingly, the N terminus alone (dZC3H3-N–v5) acts as a dominant negative, as expression of this fragment caused an exacerbation of the poly(A) RNA export defect (Fig. 1, C and D [row 2]). Despite relatively low expression levels (unpublished data), expression of dZC3H3's N terminus in GFP-depleted cells resulted in 82% of transfected cells to show a strong nuclear accumulation of poly(A) RNA, a level nearly identical to that seen upon dZC3H3 depletion. Furthermore, the localization of the N-terminal fragment was completely coincident with accumulation of poly(A) signal (Fig. 1 D, rows 1 and 2), suggesting that despite elimination of the zinc fingers, the N terminus is still able to interact either directly or indirectly with poly(A) RNA. In summary, these results indicate that the C terminus of dZC3H3 is necessary and partially sufficient for nuclear poly(A) RNA export.

Distinct domains of dZC3H3 differ in their ability to interact with NXF1

A previous study has indicated that dZC3H3 physically interacts with the essential export factor NXF1 (Farny et al., 2008). By assaying the propensity of the different dZC3H3 deletion mutants to coimmunoprecipitate with GFP-tagged NXF1, we identified the most significant interactions to occur between NXF1 and dZC3H3's N terminus. S2R+ cells were cotransfected with one of the three dZC3H3 constructs (FL-v5 [full length], N-v5 [N terminal], and C-v5 [C terminal]) or l(1)10Bb-v5 (lethal (1)10Bb), a factor previously determined to not interact with NXF1 (Farny et al., 2008), and either GFP-NXF1 or GFP. Co-immunoprecipitation (co-IP) results illustrate that all three versions of dZC3H3 interact with NXF1, albeit to different extents (Fig. 2 A). l(1)10Bb-v5 did not show interaction with NXF1 (Fig. 2 A) nor did GFP alone significantly interact with any of the dZC3H3 constructs (not depicted). Quantification of the fraction of input v5 protein that immunoprecipitated with GFP-NXF1 reveals that the N-terminal portion of dZC3H3 interacts more strongly with GFP-NXF1 (5–15-fold) than does the full-length form (Fig. 2 B). These results suggest that, in the absence of the C terminus of the protein, the N terminus of dZC3H3 may interact with NXF1 to an aberrant extent.

dZC3H3 interacts with other export factors and poly(A) RNA

To identify additional interactors of dZC3H3, we performed TAP of N- or C-terminally TAP-tagged dZC3H3 from stably integrated S2R+ cells. A two-step purification was performed using both N- and C-terminally tagged dZC3H3 lines as well as empty vector lines (to control for factors that may nonspecifically interact via the tandem affinity purification [TAP] tag), and associating proteins were identified by mass spectrometry (MS). We concluded that many proteins specifically interacted with TAP-dZC3H3, as they were not purified from the empty TAP vector cells (Fig. 3 A) or from comparable lines expressing heterologous bait proteins (not depicted). After subtraction of nonspecific interactors and common contaminants from the data, we identified 28 unique factors that interacted with dZC3H3 in at least two out of four experimental samples (see Materials and methods and Table S1). Gene ontology analysis illustrates that many of these factors (64%, $P = 4.7 \times 10^{-18}$) bind or are predicted to bind RNA, which is consistent with the hypothesis that dZC3H3 similarly plays a role in mRNA metabolism (Fig. 3 B).

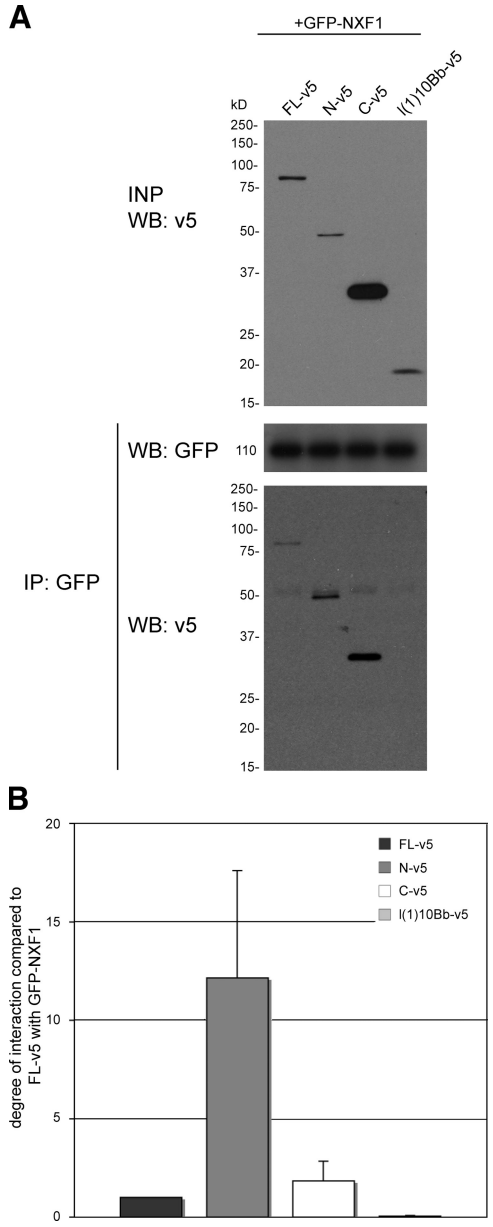

Figure 2. **dZC3H3's N terminus mediates a strong interaction with NXF1.** (A) GFP-NXF1 interacts to different degrees by co-IP with all three v5-tagged dZC3H3 deletion mutants (Fig. 1) tested. (B) The bar graph illustrates relative interaction strengths of GFP-NXF1 with the v5-tagged deletion mutants as given by a ratio of IP signal to input signal for each reaction compared with that for full-length (FL) dZC3H3. INP, input; WB, Western blot. Error bars indicate SDs of results between three experimental replicates.

Interestingly, several previously identified protein complexes were recovered with dZC3H3 in the TAP purification. The polytene chromosome puff proteins NonA (No on transient A), Hrb87f, and Pep (protein on ecdysone puffs) have been co-purified previously as a stable RNA-associated complex and were all identified in this study as dZC3H3 interactors (Reim et al., 1999). NonA has also been shown to interact with and modulate the intranuclear mobility of NXF1 (Kozlova et al., 2006).

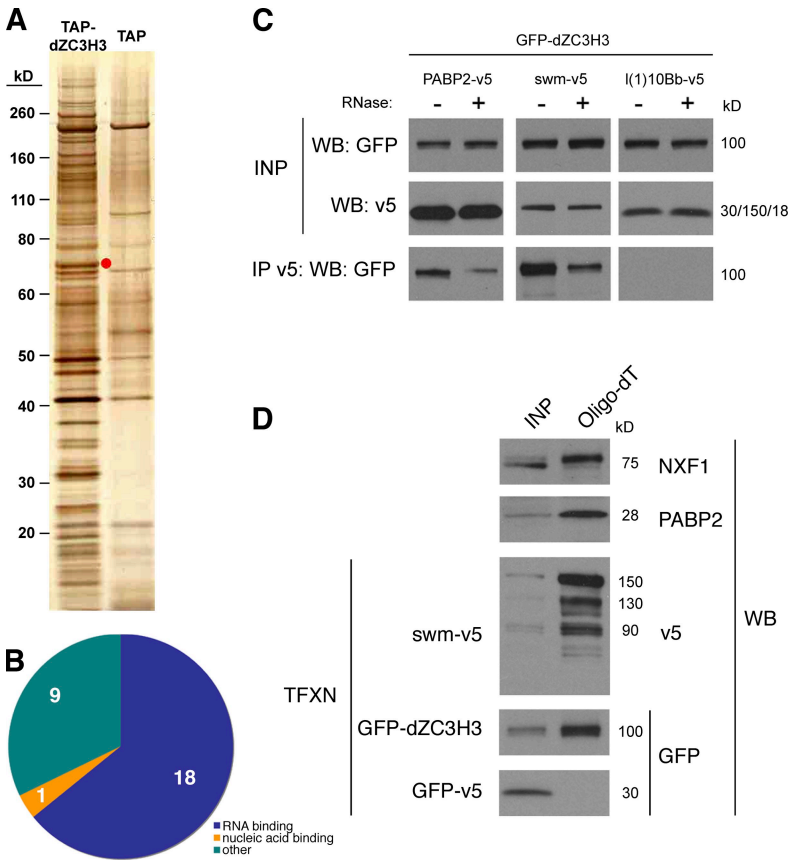

Figure 3. **dZC3H3 interacts in a complex of export factors and with poly(A) RNA.** (A) Silver-stained gel of final eluate samples from S2R+ cells that stably express TAP-dZC3H3 or TAP vector alone illustrate proteins that specifically purify with dZC3H3 (left) and not in control (right). The position of the TAP-tagged dZC3H3 bait is marked with a red dot. (B) Gene ontology analysis and domain searching reveals that 19 out of the 28 dZC3H3 interactors interact with or are predicted to interact with nucleic acids and 18 specifically with RNA. (C) Interactions of PABP2-v5 and swm-v5 with GFP-dZC3H3 are partially RNA dependent. PABP2-v5, swm-v5, or l(1)10Bb-v5 (as a negative control) were co-transfected with GFP-dZC3H3 and immunoprecipitated using v5-agarose resin in the presence or absence of RNase. (D) GFP-dZC3H3, swm-v5, NXF1, and PABP2 interact with poly(A) RNA. Nuclear poly(A) RNA was purified under nondenaturing conditions using oligo-dT cellulose resin from S2R+ cells transfected (TFXN) with GFP-dZC3H3, swm-v5, or GFP-v5 alone and analyzed by immunoblotting for associating proteins. INP, input; WB, Western blot.

The siRNA-mediated gene repression effectors AGO2 (argonaute 2), Rm62 (p68), and Fmr1 (fragile X mental retardation 1) were also isolated in the TAP-dZC3H3–containing complex, potentially indicating a link between dZC3H3's function and gene silencing (Ishizuka et al., 2002). Finally, second mitotic wave missing (swm) and PABP2 were identified as strong dZC3H3 interactors (purified 4/4 and 3/4 times, respectively). Both swm and PABP2 were recovered in our prior screen for RNA nuclear export factors and were previously isolated as interactors in a large scale two-hybrid study (Giot et al., 2003; Farny et al., 2008). Swm possesses an RNA-binding recognition motif and, like ZC3H3, a CCCH-type zinc finger region, strongly suggesting that it is an RNA-binding protein.

To confirm the interactions of dZC3H3 with swm and PABP2, co-IP reactions of these factors were conducted in the absence or presence of RNase. Fig. 3 C illustrates that GFP-dZC3H3 coimmunoprecipitates with both v5-tagged PABP2 and swm but not with tagged l(l)10Bb, thereby validating the TAP interaction data. Both interactions appear to be partially sensitive to treatment with RNase, indicating that a portion of dZC3H3's contacts with both PABP2 and swm are RNA dependent. This type of interaction is similar to that seen for GFP-NXF1 with dZC3H3-v5 (Fig. S2).

Given dZC3H3's CCCH-type zinc fingers and its interactions with export factors, including nuclear poly(A) binding protein and swm, we wanted to assess whether it associated with poly(A) RNAs. S2R+ cells were transfected with GFP-dZC3H3 or GFP-v5 alone and harvested for nuclear poly(A) RNA using an oligo-dT cellulose resin. Like endogenous PABP2 and NXF1, GFP-dZC3H3 specifically copurified with the poly(A) fraction (Fig. 3 D). Furthermore, nuclear poly(A) RNA purified from cells transfected with swm-v5 coprecipitated this factor as well, suggesting that it associates with messenger RNP particles (mRNPs; Fig. 3 D). Thus, these four factors, NXF1, PABP2, dZC3H3, and swm, associate with nuclear poly(A) RNA and may function together in transcript nuclear export.

Proper mRNA polyadenylation requires dZC3H3 activity

Given the association of dZC3H3 with PABP2, a factor required both for the polyadenylation of mRNA 3′ ends and controlling tail length, we wished to determine whether dZC3H3 functions in the polyadenylation process as well. Fig. 4 A illustrates lengths of the poly(A) tail populations of S2R+ cells that have been depleted of GFP, dZC3H3, NXF1, or Rrp6, a core component of the nuclear exosome and an mRNA export factor (Briggs et al., 1998; Farny et al., 2008). GFP-depleted control cells exhibited tail lengths of 150–200 adenines, which is consistent with the typical length of *Drosophila* mRNA poly(A) tails (Benoit et al., 2005). In contrast, cells depleted of dZC3H3, NXF1, or Rrp6 displayed an increase in tail length (Fig. 4 A). Quantification of the percentage of poly(A) tails longer than 200 adenines in each sample reflects the hyperadenylation defect that results in the absence of each of the three export factors

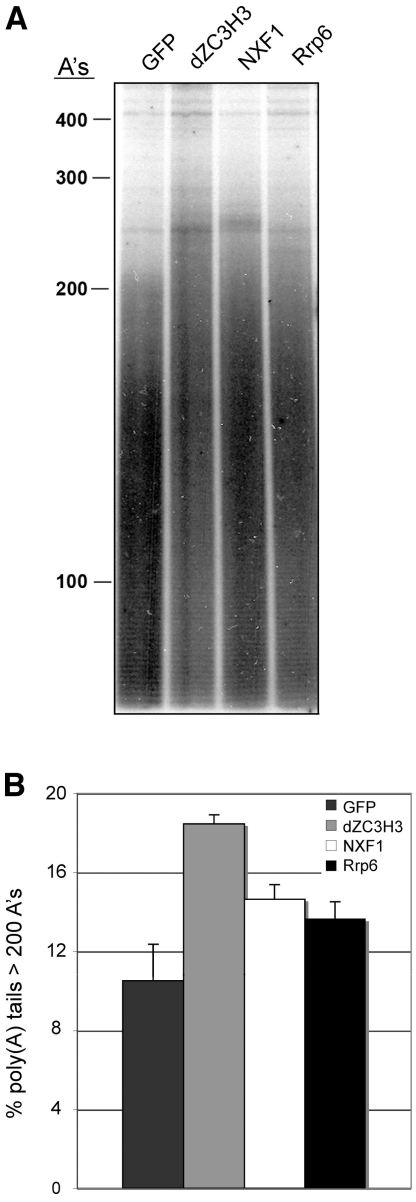

Figure 4. **Transcript hyperadenylation results upon dZC3H3 depletion.** (A) Total poly(A) RNA from cells depleted of various export factors or GFP (control) was harvested, 3′ end labeled, and digested. The sizes of remaining poly(A) tails were analyzed by TBE Urea PAGE and autoradiography. Lengths of the adenylate (A) tails were assessed by comparison to an RNA marker at left. (B) The degree of hyperadenylation was determined by calculating the percentage of total poly(A) tail signal residing above 200 nucleotides in each sample. Error bars indicate SDs of results between two experimental replicates.

(Fig. 4 B). We observed the most significant increase in tail length to occur upon depletion of dZC3H3.

ZC3H3 has a conserved role in RNA export

To determine whether the RNA export function of dZC3H3 is conserved in higher organisms, we assessed ZC3H3's requirement in the nuclear export of poly(A) RNA in the human tissue culture line U2OS. U2OS cells were transfected with siRNAs targeting the essential export factor NXF1, ZC3H3, or a nontargeting sequence (control) and 72 h later were fixed and hybridized with Cy3-OdT to visualize poly(A) RNA (Fig. 5). Widefield images in Fig. 5 A were taken using a 20× objective and a consistent exposure time to allow direct comparison of RNA in situ signals between siRNA treatments. Images in Fig. 5 (B–E) were taken using a 60× objective, and the exposure times used were adapted to the in situ signal intensity. Control cells treated with a nontargeting siRNA exhibit weak nuclear and cytoplasmic poly(A) RNA staining (Fig. 5, A and B). In contrast, upon depletion of the mRNA export factor NXF1, cells strongly accumulate poly(A) RNA within the nucleus (Fig. 5, A and C). ZC3H3 depletion also results in a robust nuclear accumulation of poly(A) RNA (Fig. 5 A). The observed subcellular poly(A) localization defects of cells depleted of NXF1 and ZC3H3 are likewise reflected by an increase in the ratio of nuclear to cytoplasmic Cy3-OdT intensity from that of control cells (Fig. S3 A). Unlike in NXF1-depleted cells, the nuclear Cy3-OdT signal of ZC3H3-depleted cells is concentrated in distinct foci (Fig. 5 D). Depletion of ZC3H3 using a second nonoverlapping siRNA resulted in a similar accumulation of poly(A) RNA, indicating the specificity of this effect (unpublished data).

In addition to bulk poly(A) RNA, specific mRNA transcripts are also sequestered in the nuclei of cells depleted of ZC3H3. We monitored the subcellular localization of endogenous *RPL32* (large ribosomal protein 32) transcripts by hybridization of U2OS cells treated with NXF1, ZC3H3, or control siRNAs with a Cy3-conjugated oligo probe complimentary to the *RPL32* mRNA (Cy3-RPL32). Additionally, to simultaneously monitor the distribution of the poly(A) RNA in these cells, we cohybridized these samples with a biotin-conjugated oligo-dT (biotin-OdT) probe. Similar to the results observed using the Cy3-OdT probe, depletion of either NXF1 or ZC3H3 from cells resulted in an increase in the nucleocytoplasmic ratio of *RPL32* signal intensity compared with control cells (Fig. S3 B). Interestingly, the poly(A) foci of ZC3H3-depleted cells additionally contain *RPL32* mRNA, whereas the nuclear *RPL32* signal is more diffusely distributed in NXF1-depleted cells (Fig. 5 E). Thus, ZC3H3 function is required for export of poly(A) RNAs, at least a subset of which are mRNAs, from the nuclei of human cells. However, ZC3H3's specific activity appears to differ from that of the core export factor NXF1.

ZC3H3 functions downstream of nuclear poly(A) binding protein (PABPN1)

Given dZC3H3's interactions with PABP2 and its polyadenylation-related function in the fly, we wished to assess ZC3H3's relationship to the human form of this factor (PABPN1). Similar to its fly counterpart, PABPN1 is required for efficient poly(A) tail synthesis as well as poly(A) tail length control (Wahle, 1995). To assess the effect of PABPN1's activity on the localization of poly(A) RNA, the Cy3-OdT in situ staining pattern of PABPN1-depleted U2OS cells was determined and compared with that of ZC3H3-depleted cells. As described previously, images of cells treated with various siRNAs were processed for poly(A) RNA in situ staining and photographed to enable comparison of nuclear poly(A) signal intensities between knockdown samples (Fig. 6 A). Quantification of the percentage of cells within a population that exhibit a nuclear poly(A) signal intensity over a baseline threshold

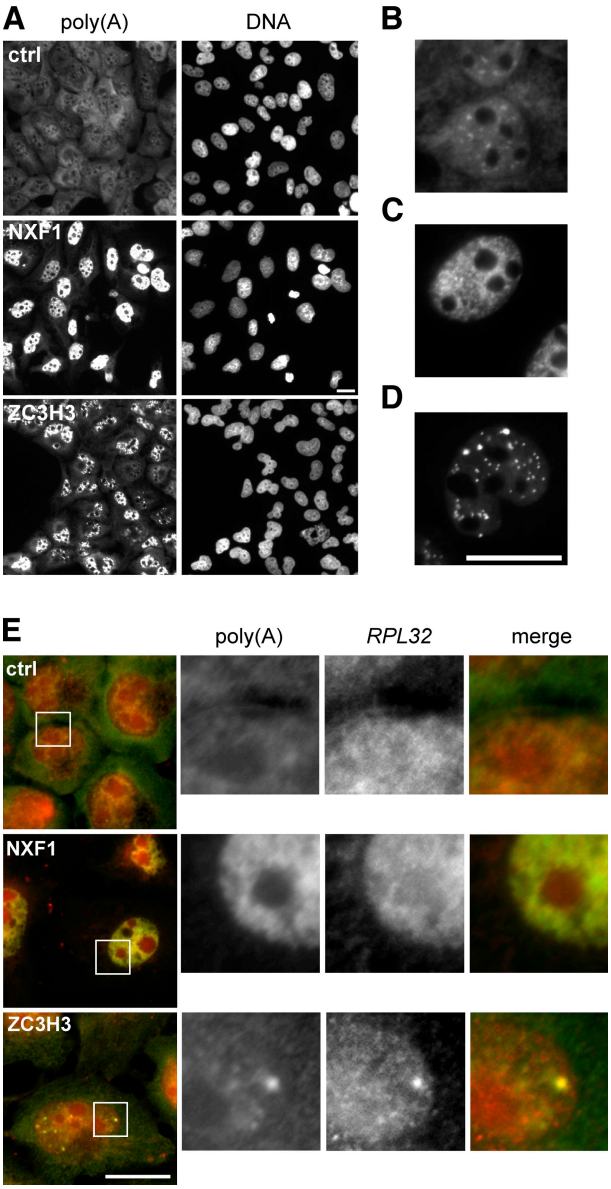

Figure 5. **Function of ZC3H3 in mRNA nuclear export is conserved in humans.** (A) U2OS cells were treated with control (ctrl) siRNAs or siRNAs targeting NXF1 or ZC3H3 for 3 d and fixed, permeabilized, hybridized with Cy3-OdT (left) to visualize poly(A) RNA, and stained for DNA (right). Images were taken using equivalent exposure times in the Cy3 channel (poly(A) RNA) to enable comparison of signal level between samples. Note the saturation of nuclear pixels in NXF1- and ZC3H3-depleted cells that results from the use of exposure times long enough to visualize poly(A) RNA signal in control cells. Poly(A) localization was further inspected in control cells (B), NXF1-depleted cells (C), and ZC3H3-depleted cells (D). (E) *RPL32* mRNA and poly(A) RNA was visualized by hybridization of control, NXF1-, or ZC3H3- depleted cells with Cy3-RPL32 (red) and biotin-OdT (green) probes. Images within the white boxes are magnified at right. Bars, 20 µm.

was used to compare the level of nuclear poly(A) accumulation in each treatment (Fig. 6 B). As anticipated from our results in Fig. 5, depletion of ZC3H3 results in a dramatic increase in the degree of cells exhibiting a high level of nuclear signal compared with control cells (Fig. 6 B). Treatment of cells with siRNAs targeting PABPN1 results in a reduction in the percentage of cells possessing a high level of nuclear poly(A) RNA. This decrease is likely indicative of PABPN1's requirement in the polyadenylation reaction and the cells' impaired ability to processively polyadenylate transcripts in its absence (Fig. 6, A and B). Interestingly, simultaneous reduced expression of ZC3H3 and PABPN1 causes cells to no longer demonstrate the high nuclear poly(A) signals characteristic of those depleted of ZC3H3. Instead, codepletion of ZC3H3 and PABPN1 results in penetrance of nuclear poly(A) accumulations indistinguishable from those of PABPN1 knockdown cells. Assessment of the efficiency of ZC3H3 and PABPN1 protein depletion in each sample indicates that this result is not a consequence of inefficient ZC3H3 knockdown (Fig. 6 C). The reversal of poly(A) signal accumulation upon codepletion of ZC3H3 and PABPN1 indicates that these two factors function in the same adenylation pathway and that PABPN1 activity is upstream of that of ZC3H3.

Depletion of ZC3H3 results in an aberrant spatial distribution of nuclear poly(A) RNA

The punctate pattern of poly(A) accumulation resultant in ZC3H3-depleted cells led us to question whether these foci were coincident with any known nuclear bodies. Costaining of the poly(A) RNA and coilin or promyelocytic leukemia protein, markers of Cajal and promyelocytic leukemia bodies, respectively, in ZC3H3-depleted cells revealed no significant colocalization (unpublished data). Similarly, visualization of paraspeckles (using a fluorescently tagged version of PSP1α [paraspeckle protein 1α] did not demonstrate significant overlap with the accumulated RNA (Fig. S4). However, inspection of the localization of poly(A) accumulations and nuclear speckles, as indicated by the splicing factor and speckle component SC35, illustrated that depletion of ZC3H3 causes a change in the spatial relationship between these two domains (Fig. 6 D). Mammalian cell nuclei normally contain a basal level of nuclear poly(A) RNA with specific accumulations within nuclear speckle domains (Carter et al., 1991). Strikingly, abrogation of ZC3H3 expression in these cells results in nuclear poly(A) foci that are removed from and proximal to these speckle domains. Thus, depletion of ZC3H3 results in either an aberrant accumulation or redistribution of nuclear poly(A) RNA from within the SC35-containing speckles to regions just outside of these domains.

Unexpectedly, closer inspection of cells depleted of PABPN1 revealed that the nuclear poly(A) in situ signal, although of very weak intensity and more fractured than in ZC3H3-depleted cells, is similarly aberrantly distributed in punctate foci (Fig. 6 D). Diminished PABPN1 expression results in nuclear poly(A) signals and SC35 staining that is more coincident than in ZC3H3 siRNA–treated cells but less coincident than in cells treated with control siRNAs. As in Fig. 6 B, codepletion of ZC3H3 and PABPN1 results in foci with similar properties to those of cells depleted only of PABPN1 (Fig. 6 D).

Given PABPN1's polyadenylation-related functions and its requirement for the formation of the poly(A) foci observed upon dZC3H3 depletion, we investigated whether it colocalized with these poly(A) accumulations. Normally, PABPN1 primarily resides in the nucleus with specific concentrations within the nuclear speckles (Krause et al., 1994). However, similar to the redistribution of intranuclear poly(A) RNA, PABPN1's subnuclear localization is altered upon ZC3H3 depletion, causing a

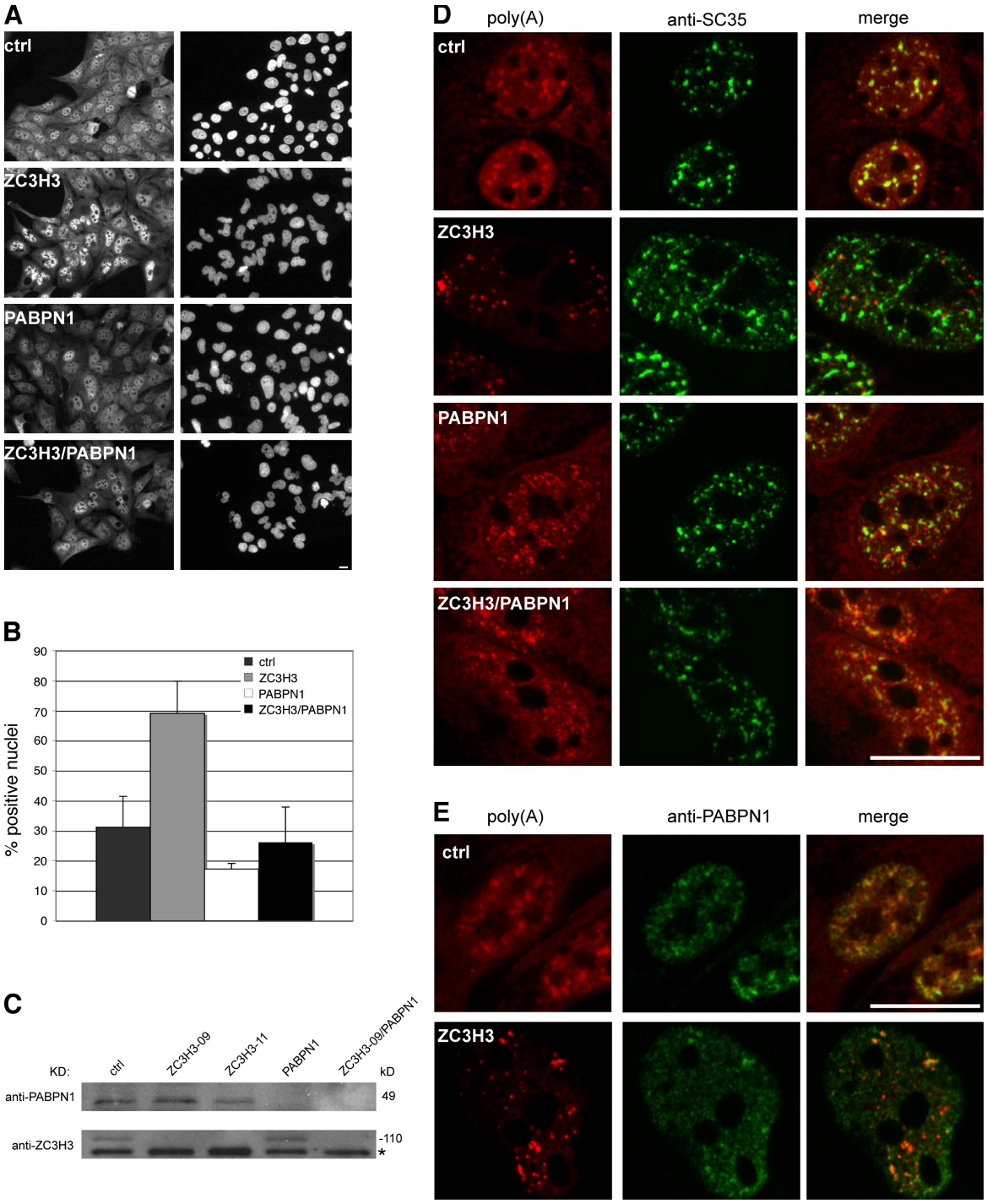

Figure 6. **ZC3H3 modulates mRNA polyadenylation downstream of PABPN1 activity.** (A) U2OS cells were monitored for poly(A) RNA localization by hybridization with Cy3-OdT probe (left) as in Fig. 5 after depletion with either control siRNAs (ctrl) or siRNAs targeting ZC3H3, PABPN1, or both. Images acquired in the Cy3 channel (poly(A) RNA) were captured using equivalent exposure times to allow comparison of signal intensity between samples. (B) Quantification of the percentage of cells possessing nuclear poly(A) signal over background for cells treated as in A illustrates that codepletion of ZC3H3 and PABPN1 results in a nuclear accumulation phenotype indistinguishable from control. (C) Immunoblot demonstrating efficient depletion of siRNA-targeted factors in A. A nonspecific protein interaction occurs with anti-ZC3H3 antibodies (asterisk) in all samples, indicating equivalent protein loading between lanes. ZC3H3-11 is a second siRNA targeting ZC3H3 that was used to deplete cells. (D) A change in the localization of nuclear poly(A) RNA (Cy3-OdT, red) with respect to nuclear speckles (SC35, green) is resultant in ZC3H3-, PABPN1-, and ZC3H3/PABPN1-depleted samples as compared with control cells. (E) PABPN1 (green) colocalizes with poly(A) RNA (red) in both control and ZC3H3-depleted cells. Images in D and E were captured using confocal microscopy. Bars, 20 µm.

significant portion of the protein to colocalize with the resultant poly(A) foci (Fig. 6 E). These results further support a function for PABPN1 in the formation and/or maintenance of these nuclear poly(A) RNA foci.

To further investigate the relationship between nuclear speckles and poly(A) RNA foci in ZC3H3-depleted cells, we monitored their relative localization in ZC3H3-depleted or control cells that had been treated with the RNA polymerase II–specific transcriptional inhibitor α-amanitin. Transcriptional inhibition causes enlargement and rounding of the nuclear speckles as has been observed previously (Fig. 7; Huang et al., 1994). However, this morphological change does not disrupt the colocalization of nuclear poly(A) and SC35 staining in control cells (Fig. 7, row 2, inset). α-Amanitin treatment of ZC3H3-depleted cells does not disrupt the presence of the poly(A) foci, indicating that ongoing transcription is not required for their maintenance. However, under these conditions, the poly(A) foci in ZC3H3-depleted cells accumulate around the periphery of the SC35 domains, sometimes completely surrounding the speckles (Fig. 7, row 4, inset).

Discussion

Despite significant evidence, particularly in yeast, indicating that mRNA 3′ end processing and nuclear export are coupled, relatively little is understood about the coordination, both spatially and mechanistically, of these two events. In this study, we show that *Drosophila* factor dZC3H3 is required for both the proper polyadenylation and export of mRNAs. Cells depleted of dZC3H3 have longer poly(A) tails and exhibit a nuclear poly(A) phenotype. Consistent with these findings, we identify the polyadenylation factor PABP2 as a dZC3H3 interactor. We dissect the domains of dZC3H3 and discover that its C terminus is required for its export activity. We also show that the human homologue of this factor, ZC3H3, is similarly required for proper nuclear export of adenylated transcripts, as its depletion results in the formation of nuclear poly(A) RNA foci peripheral to nuclear speckles in U2OS cells. Formation of these foci is dependent on PABPN1 function, further suggesting the conservation of ZC3H3's function between organisms.

The N- and C-terminal domains of dZC3H3 mediate the export of poly(A) RNA to different extents. The dominant-negative effect of expressing dZC3H3's N terminus on RNA export suggests that the C terminus is required to keep dZC3H3 function, such as interaction with NXF1, in check. Additionally, in the absence of the C terminus, the N-terminal segment of dZC3H3 may be unable to modify the messages properly, thereby preventing their export via activation of additional surveillance mechanisms (Fig. 1 D).

We have now demonstrated physical interactions between dZC3H3 and three other factors, NXF1, PABP2, and swm, all of which are similarly required for mRNA nuclear export. These factors may function together or in combination in a larger mRNA export-associated complex. RNase sensitivity assays revealed that all of these interactions are dependent on the presence of RNA to varying degrees (Fig. 3 C and Fig. S2). Therefore, it is likely that either some of these factors do not directly contact each other but are tethered together via a common RNA molecule or that their interactions with each other are dependent on changes in protein conformations induced upon their association with RNA. Indeed, specific protein conformational changes have been observed for the CCCH-type zinc finger protein tristetraprolin upon RNA binding (Brewer et al., 2004).

We show that absence of ZC3H3 causes the appearance of aberrant poly(A) foci peripheral to nuclear speckles. We have also demonstrated that at least some of these accumulated poly(A) RNAs are mRNA molecules normally destined for export but abnormally retained due to depletion of this factor. Although the nuclear speckle is widely regarded as a compartment integral to mRNA processing, its exact functional and spatial relation to mRNAs is not clearly defined. Significant evidence indicates that a speckle-localized poly(A) RNA is dynamically associated with these domains (Molenaar et al., 2004; Politz et al., 2006; Ishihama et al., 2008). Indeed, some mRNA transcripts have been shown to transit through speckles before their export (Smith et al., 1999). However, this phenomenon appears to be transcript specific, as other messages have only ever been observed at the periphery of speckles (Smith et al., 1999). The poly(A) accumulations resultant upon ZC3H3 depletion may represent transcripts that are forming at the periphery of these domains.

Alternatively, these foci could be indicative of adenylated transcripts that normally transit through speckles but are instead trapped upon entry or exit from these domains. Interestingly, *DMPK* (*dystrophia myotonica protein kinase*) mRNA normally travels through the speckle before its export. However, in myotonic dystrophy I patient myoblasts, which harbor an abnormal CUG triplet expansion in the 3′ untranslated region of the *DMPK* gene, this message is trapped just outside of the speckle and is not exported from the nucleus (Smith et al., 2007). Depletion of ZC3H3 may be causing a similar but more widespread problem in speckle trafficking of mRNAs.

Previous work has demonstrated that transcripts that are aberrantly trapped in the nucleus, resulting from improper mRNP formation, are often specifically retained at their site of transcription (Long et al., 1995; Custodio et al., 1999; Brodsky and Silver, 2000). Thus, misprocessed messages may be tethered to a site where they can be monitored by surveillance factors (for reviews see Saguez et al., 2005; Schmid and Jensen, 2008). Some evidence suggests that mRNAs are transcribed in regions peripheral to speckle domains (Xing et al., 1995; Cmarko et al., 1999). In cells depleted of ZC3H3, transcriptional inhibition results in concurrent morphological changes in both speckle shape and foci organization, suggesting a physical and/or functional link between these two features. These poly(A) foci potentially indicate sites of cotranscriptional mRNA processing activity, containing transcripts stalled at a stage during polyadenylation just before export. ZC3H3 may be required to interact productively with mRNPs to signal that the message is properly adenylated and ready for release from its site of transcription for export (Fig. 8). Consistent with this model, dZC3H3 interacts with Rm62, which in addition to having a role in gene silencing, was also found to be required for proper clearance of *HSP70* mRNAs from their transcriptional locus after heat shock (Buszczak and Spradling, 2006).

Although 3′ end processing defects can inhibit transcript nuclear export, mutations in export factors can also cause

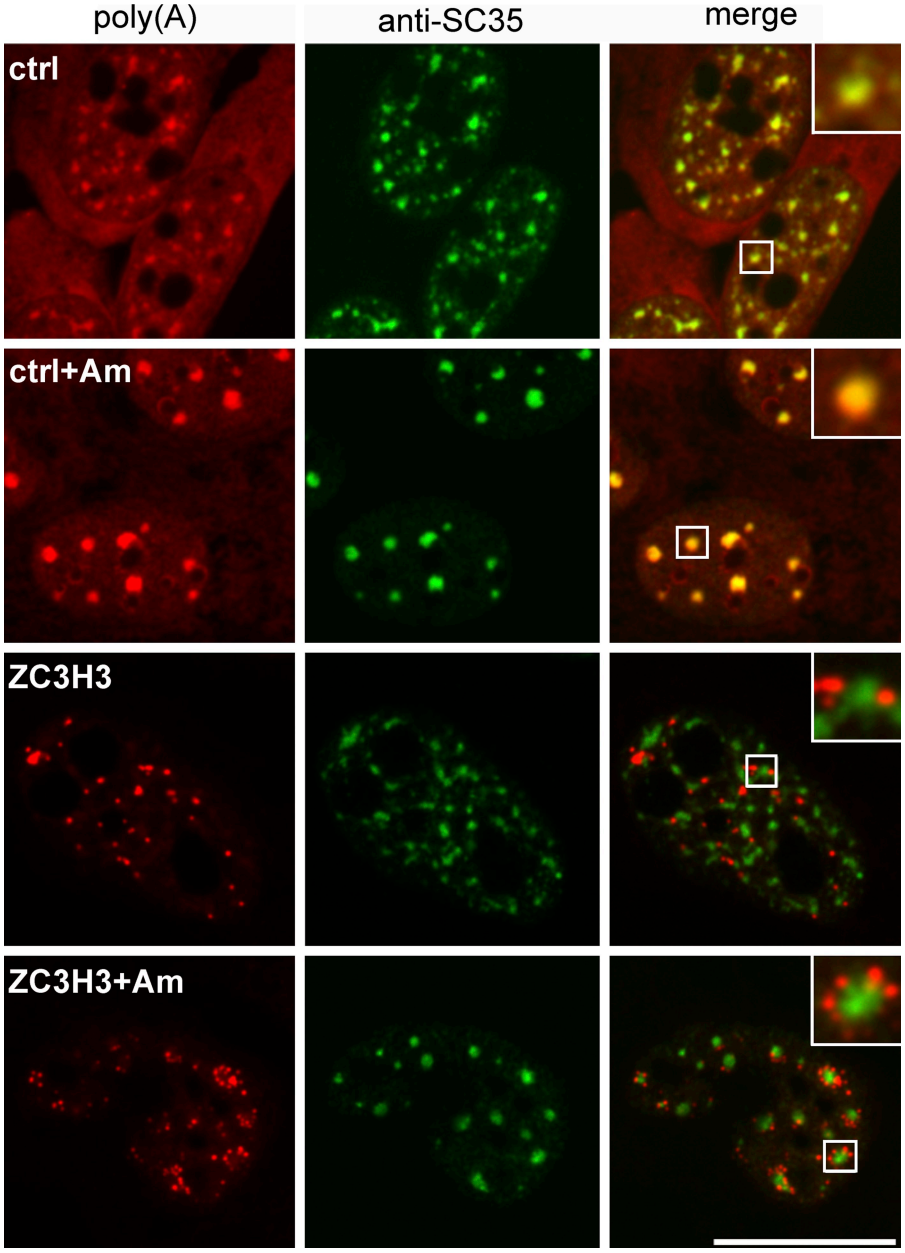

Figure 7. **ZC3H3-dependent nuclear poly(A) RNA accumulations respond to transcriptional inhibition.** Confocal images of U2OS cells that were treated with control (ctrl) siRNAs or siRNAs targeting ZC3H3 for 3 d and incubated with or without 50 ug/ml α-amanitin (Am) for 6 h before fixation, permeabilization, hybridization with Cy3-OdT probe, and immunostaining with anti-SC35 antibodies. Merged images within white boxes are enlarged at the top right to enable better resolution of features. Bar, 20 µm.

aberrations in transcript 3′ end formation. For example, mutations in yeast export factors, including Mex67p, Gle1p, and Sub2p result in polyadenylation defects, specifically hyperadenylation (Hilleren and Parker, 2001; Jensen et al., 2001). However, in contrast to transcript hyperadenylation resulting from export defects in ZC3H3-depleted cells, we favor a model in which ZC3H3 functions directly in the polyadenylation process for several reasons: (1) depletion of dZC3H3 results in a more significant effect on poly(A) tail length (1.8-fold increased over control cells) than does either NXF1 or Rrp6 (a known RNA nuclease), (2) dZC3H3 interacts physically with PABP2, (3) dZC3H3 has homology to a 3′ end processing subunit, clp, and (4) formation of aberrant poly(A) foci in the absence of ZC3H3 requires the activity of PABPN1. Whether the trapping of mRNAs in the nucleus upon dZC3H3 depletion is caused by a second export-related function of dZC3H3 (perhaps via interaction with NXF1) or is rather a downstream consequence of improper 3′ end polyadenylation and enactment of nuclear surveillance machinery is unknown. However, it should be noted that export defects were not observed upon depletion of many 3′ end processing factors (Farny et al., 2008).

What is dZC3H3's function in the polyadenylation process? We envision the following three nonmutually exclusive scenarios (Fig. 8). First, ZC3H3 may be required to release transcripts from their site of transcription after proper polyadenylation has taken place. Second, this factor may aid in poly(A) tail length control by facilitating the release of other adenylation factors. Third, ZC3H3 may play a role in trimming the poly(A) tail down to the appropriate length. Indeed, Collart et al. (2005a) illustrated that mouse Zc3h3 possesses nuclease activity in vitro using a radiolabeled RNA template.

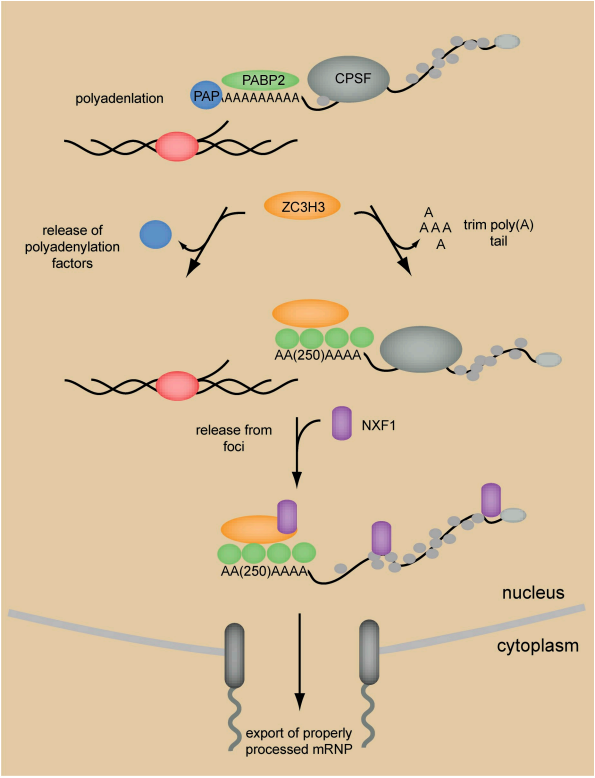

Figure 8. **Model of potential roles of ZC3H3 in polyadenylation and nuclear export.** RNA processing factors (light gray) are recruited to mRNAs during transcription by RNA polymerase II (red). During the processive stage of polyadenylation, CPSF (dark gray) and PABP2 (green) tether PAP (blue) to the elongating tail. ZC3H3 (orange) may aid in the recognition of tails of the proper length, trim the tail to the proper length, or release polyadenylation factors (such as PAP) after the proper length has been attained. This activity could additionally aid in the release of the poly(A) transcript from the transcription focus, thereby allowing it to proceed toward the nuclear periphery for export via interactions with export factors such as NXF1 (purple). For simplicity, ZC3H3 is shown to interact with the mRNP after the initiation of transcript polyadenylation. However, it is possible that this factor is recruited to transcripts before polyadenylation but functions at a later stage in mRNA biogenesis.

In this study, we have characterized a novel CCCH-type zinc finger protein and illustrated its importance in both the adenylation and export of metazoan nuclear mRNAs. We have further provided clues to the linkage between these two processes, as depletion of this factor causes unusual accumulations of adenylated RNA at the periphery of nuclear speckles, a domain whose functional role is tied to RNA processing. These data are consistent with a model in which ZC3H3 is required for release of adenylated transcripts from their processing centers, adjunct to nuclear speckles, en route to export.

Materials and methods

Cell lines and constructs

Drosophila S2R+ cells were maintained in Schneider's *Drosophila* medium (Invitrogen) containing 10% FBS and penicillin/streptomycin solution. Full coding regions of genes (as given by FlyBase) were cloned by RT-PCR from total RNA isolated from S2R+ cells and inserted into pAc5.1-v5/His (Invitrogen) or pAc5.1 containing an N-terminal GFP. dZC3H3 deletion mutants were constructed as follows: dZC3H3-FL, aa 1–597; dZC3H3-N, aa 1–388; dZC3H3-C, aa 389–597. pEYFP-C1-PSP1α was provided by D. Spector (Cold Spring Harbor Laboratories, Cold Spring Harbor, NY). For TAP experiments, the full coding region of dZC3H3 was cloned into each of pMK33-N-TAP and pMK33-C-TAP (Veraksa et al., 2005). A stable cell line was generated for each dZC3H3 construct as well as each empty pMK33 vector by selection in media containing 300 µg/ml Hygromycin B (Invitrogen; Veraksa et al., 2005). For human cell experiments, U2OS cells were maintained in DME containing 10% FBS and penicillin/streptomycin solution.

Poly(A) length analysis

Poly(A) tails were analyzed essentially as described previously (Perreault et al., 2007). In brief, total RNA was harvested from *Drosophila* S2R+ cells that had been depleted using dZC3H3, NXF1, Rrp6, or GFP-targeting dsRNAs. 2.5 ug total RNA from each sample was 3′ end labeled with [^{32}P]pCp followed by digestion with RNase A and T1. A mixture of RNA standards (RNA Century-plus; Applied Biosystems) was similarly labeled and processed for size comparison. Products were separated on TBE Urea polyacrylamide gels, imaged by autoradiography, and quantified using Quantity One software (Bio-Rad Laboratories).

Drosophila RNAi, transfections, and fluorescence microscopy

For dual transfection and knockdown experiments, S2R+ cells were first transfected with v5-tagged deletion constructs of the CG6694 coding sequence or GAPDH1 for 24 h and knocked down for an additional 48 h with either a dsRNA targeting the N-terminal (DRSC31743) or C-terminal (DRSC31742) portion of the CG6694 mRNA or GFP mRNA. In situ samples were fixed and hybridized using a Cy3-OdT(30) probe (Integrated DNA Technologies) followed by staining with mouse anti-v5 (Abcam) and Alexa Fluor 488 donkey anti–mouse (Invitrogen) or Alexa Fluor 488–conjugated wheat germ agglutinin (Invitrogen) as described previously (Farny et al., 2008). Images were captured using confocal microscopy, and transfected cells (n > 40) were scored blindly for nuclear accumulation of poly(A) mRNA. This experiment was repeated three times.

IP experiments

Anti-GFP IP experiments were performed as described previously (Farny et al., 2008) except that precleared lysates were incubated overnight with 3.6 ug rabbit anti-GFP antibody and immunoprecipitated for 4 h using protein A–Sepharose beads (GE Healthcare). For RNase experiments, samples were harvested in lysis buffer (50 mM Tris, pH 7.5, 1.5 mM $MgCl_2$, 125 mM NaCl, 0.2% NP-40, 5% glycerol, 1 mM EDTA, and protease inhibitors) and treated with or without RNase cocktail (Applied Biosystems) for 30 min at room temperature before preclearing and IP using v5-agarose beads (Sigma-Aldrich). After washing with lysis buffer, purified samples were analyzed by Western blotting using either mouse anti-v5 (Invitrogen) or rabbit anti-GFP antibody. Quantification of interaction strength between dZC3H3 mutants and GFP-NXF1 was performed using Quantity One software by taking a ratio of the IP signal to the INPUT signal for each reaction and normalized to that of full-length dZC3H3 with GFP-NXF1.

TAP and MS analysis

Stable S2R+ cell lines were induced to produce each TAP fusion protein by treatment with media containing 0.21 mM cupric sulfate for 20 h. Cells were lysed, and TAP was performed as described previously (Veraksa et al., 2005), wherein lysates were first subjected to purification over IgG-Sepharose beads, and tobacco etch virus protease cleavage eluates were further purified over calmodulin-Sepharose beads. Peptides were generated from purified samples by in-solution trypsin digestion and analyzed by liquid chromatography MS/MS. Spectra were analyzed using the SEQUEST algorithm against the *Drosophila* protein database, and all identified peptides were filtered by tryptic state, XCorr, and dCorr. A factor was identified as a dZC3H3 interactor if its corresponding peptides were not isolated in any of the control purifications nor identified in any previous study as common contaminants of the *Drosophila* TAP/liquid chromatography MS/MS procedure, and either the factor was identified in three out of four or two out of the four experimental purifications and by at least two unique peptides. Gene ontology analysis was performed using DAVID Bioinformatics Resources 2008 web-based tool (http://david.abcc.ncifcrf.gov/; Dennis et al., 2003). The RNA-binding protein enrichment p-value was derived by comparison of those found within the 28 dZC3H3 interactors to the number expected by chance in the entire *Drosophila* proteome.

Poly(A) RNA isolation

1.2 × 10^7 S2R+ cells were transfected with GFP- or v5-tagged constructs for ∼40 h and harvested for poly(A) RNA IP essentially as described previously (Kozlova et al., 2006), except PMSF was added to buffers and 0.2U/µl RNaseOUT (Invitrogen) was used as RNase inhibitor. After resuspension of precipitated proteins in sample buffer, 1/4 of the eluate sample

and 1/40 of the input samples were analyzed by SDS-PAGE followed by immunoblotting using anti-v5, anti-GFP, rabbit anti–*Drosophila* PABP2 (provided by M. Simonelig, Institut de Génétique Humaine, Montpellier, France), or rat anti–*Drosophila* NXF1 (provided by E. Izaurralde, Max Planck Institute for Developmental Biology, Tübingen, Germany).

siRNA-mediated knockdowns

1.2×10^4 U2OS cells were seeded on coverslips overnight and transfected with either 20 nM ZC3H3 (SMARTpool, ZC3H3-09, or ZC3H3-11), 20 nM PABPN1 (SMARTpool), 5 nM NXF1 (SMARTpool), or 20 nM control (siControl #2) siRNAs (Thermo Fisher Scientific) for 72 h using Hiperfect (QIAGEN) as per the manufacturer's directions. The sense strand sequences of ZC3H3-09 and ZC3H3-11 are 5′-GUUGUGACCUGUCGAACUAUU-3′ and 5′-CAAUAAAGGUUCUAUCCGAUU-3′, respectively. For dual ZC3H3/PABPN1 knockdowns, 20 nM each siRNA or mixture was used.

Mammalian RNA in situ hybridization

For sole poly(A) RNA localization analysis, U2OS cells were fixed, permeabilized, and hybridized with Cy3-OdT as described previously (Farny et al., 2008). Costaining for splicing speckles and PABPN1 was performed using mouse anti-SC35 (Abcam) and Alexa Fluor 488 donkey anti–mouse (Invitrogen) or rabbit anti–bovine PABPN1 (provided by E. Wahle, Martin Luther University Halle-Wittenberg, Halle, Germany) and Alexa Fluor 647 goat anti–rabbit (Invitrogen) after Cy3-OdT probe hybridization. For specific transcript localization, cells were fixed for 15 min in 4% paraformaldehyde/PBS and permeabilized first for 10 min in 0.5% Triton X-100 and then overnight in 70% ethanol. Cells were washed in 2× SSC/25% formamide for 5 min at room temperature before hybridization with 25 ng Cy3-RPL32 (Cy3, 5′-GGGTTATAGGAGACTGAAAGTGCTTTTCCAGTTAACCGTGGTG-GATTA-3′; Integrated DNA Technologies) and biotin-conjugated OdT(50) (1:1,000; Integrated DNA Technologies) in hybridization buffer (10% dextran sulfate, 2 mM ribonucleoside–vanadyl complex [New England Biolabs, Inc.], 0.005% BSA, 1 mg/ml yeast tRNA [Ambion], and 25% formamide in 2× SSC) for 10 min at 60°C followed by overnight at 42°C. Cells were washed once in 25% formamide/4× SSC and twice in 25% formamide/2× SSC at 42°C for 10 min each before staining with Hoechst stain and Alexa Fluor 488–conjugated streptavidin (1:1,000; Invitrogen) for 1 h in 0.1% NP-40/2× SSC. Cells were finally washed three times in 2× SSC for 5 min before mounting. MetaMorph imaging software (MDS Analytical Technologies) was used to segment individual widefield images and record area and signal intensity values for each cell and its corresponding nucleus. After local background correction, the mean nuclear and cytoplasmic signal for each cell was calculated, and a corresponding nuclear/cytoplasmic signal ratio was recorded.

Protein levels were assessed by immunoblotting using either rabbit anti–bovine PABPN1 or rabbit anti-ZC3H3 (peptide antibody generated in this study; Open Biosystems). For transcriptional inhibition experiments, U2OS cells were incubated with 50 ug/ml α-amanitin (Sigma-Aldrich) for 6 h after knockdown and before fixation and hybridization.

Image aquisition

Widefield images were acquired using MetaMorph software and a microscope (Eclipse TE2000-E; Nikon) outfitted with a charge-coupled device camera (ORCA-ER; Hamamatsu Photonics). Spinning-disk confocal images were similarly acquired using a microscope (Eclipse TE2000-U; Nikon) outfitted with a laser (70c; Innova). Images of human cells were taken using either of two objectives, Plan Apo 60×/1.40 oil (Nikon) or Plan Fluor 20×/0.5 (Nikon). Images of *Drosophila* cells were taken using a Plan Apo 100×/1.4 oil objective (Nikon). Figures were prepared using Photoshop and Illustrator (Adobe). Any γ adjustments made to images strictly followed quantitative measurements to facilitate resolution of nuclear features observed in the raw images.

Online supplemental material

Fig. S1 demonstrates that overexpression of full-length dZC3H3-v5 does not cause a poly(A) RNA nuclear export defect. Fig. S2 illustrates that dZC3H3 interacts with GFP-tagged NXF1 in an RNA-dependent manner. In Fig. S3, we show that the ratios of nuclear/cytoplasmic poly(A) RNA and *RPL32* mRNA are generally increased in both NXF1- and ZC3H3-depleted cells as compared with those of control cells. In Fig. S4, we show that the nuclear poly(A) RNA foci resultant in ZC3H3-depleted cells do not significantly colocalize with paraspeckles given by PSP1α. Table S1 shows the complete list of dZC3H3 interactors identified in this study (see TAP and MS analysis). Online supplemental material is available at http://www.jcb.org/cgi/content/full/jcb.200811072/DC1.

We thank N. Kedersha, F. Bachand, and D. Spector for protocols, reagents and advice, E. Izaurralde, M. Simonelig, and E. Wahle for antibodies, and A.E. McKee and M.J. Moore for discussion and critical reading of this manuscript. J.A. Hurt designed and performed all experiments except TAP (R.A. Obar) and MS (B. Zhai). N.G. Farny assisted with fly RNA fluorescence in situ hybridization experiments and construct generation. All authors contributed to discussion of the results and writing the manuscript.

This work was supported by grants from the National Institutes of Health to P.A. Silver (grant GM057476), R.A. Obar (grant 5R01 HG003616-04), and S.P. Gygi (grant HG3616).

Submitted: 14 November 2008
Accepted: 18 March 2009

References

Bai, C., and P.P. Tolias. 1996. Cleavage of RNA hairpins mediated by a developmentally regulated CCCH zinc finger protein. *Mol. Cell. Biol.* 16:6661–6667.

Benoit, B., G. Mitou, A. Chartier, C. Temme, S. Zaessinger, E. Wahle, I. Busseau, and M. Simonelig. 2005. An essential cytoplasmic function for the nuclear poly(A) binding protein, PABP2, in poly(A) tail length control and early development in *Drosophila*. *Dev. Cell.* 9:511–522.

Bernardi, R., and P.P. Pandolfi. 2007. Structure, dynamics and functions of promyelocytic leukaemia nuclear bodies. *Nat. Rev. Mol. Cell Biol.* 8:1006–1016.

Bienroth, S., W. Keller, and E. Wahle. 1993. Assembly of a processive messenger RNA polyadenylation complex. *EMBO J.* 12:585–594.

Brawerman, G. 1981. The role of the poly(A) sequence in mammalian messenger RNA. *CRC Crit. Rev. Biochem.* 10:1–38.

Brewer, B.Y., J. Malicka, P.J. Blackshear, and G.M. Wilson. 2004. RNA sequence elements required for high affinity binding by the zinc finger domain of tristetraprolin: conformational changes coupled to the bipartite nature of Au-rich MRNA-destabilizing motifs. *J. Biol. Chem.* 279:27870–27877.

Briggs, M.W., K.T. Burkard, and J.S. Butler. 1998. Rrp6p, the yeast homologue of the human PM-Scl 100-kDa autoantigen, is essential for efficient 5.8 S rRNA 3′ end formation. *J. Biol. Chem.* 273:13255–13263.

Brodsky, A.S., and P.A. Silver. 2000. Pre-mRNA processing factors are required for nuclear export. *RNA.* 6:1737–1749.

Buszczak, M., and A.C. Spradling. 2006. The *Drosophila* P68 RNA helicase regulates transcriptional deactivation by promoting RNA release from chromatin. *Genes Dev.* 20:977–989.

Carter, K.C., K.L. Taneja, and J.B. Lawrence. 1991. Discrete nuclear domains of poly(A) RNA and their relationship to the functional organization of the nucleus. *J. Cell Biol.* 115:1191–1202.

Cheng, H., K. Dufu, C.S. Lee, J.L. Hsu, A. Dias, and R. Reed. 2006. Human mRNA export machinery recruited to the 5′ end of mRNA. *Cell.* 127:1389–1400.

Cmarko, D., P.J. Verschure, T.E. Martin, M.E. Dahmus, S. Krause, X.D. Fu, R. van Driel, and S. Fakan. 1999. Ultrastructural analysis of transcription and splicing in the cell nucleus after bromo-UTP microinjection. *Mol. Biol. Cell.* 10:211–223.

Collart, C., J.E. Remacle, S. Barabino, L.A. van Grunsven, L. Nelles, A. Schellens, T. Van de Putte, S. Pype, D. Huylebroeck, and K. Verschueren. 2005a. Smicl is a novel Smad interacting protein and cleavage and polyadenylation specificity factor associated protein. *Genes Cells.* 10:897–906.

Collart, C., K. Verschueren, A. Rana, J.C. Smith, and D. Huylebroeck. 2005b. The novel Smad-interacting protein Smicl regulates Chordin expression in the *Xenopus* embryo. *Development.* 132:4575–4586.

Custodio, N., M. Carmo-Fonseca, F. Geraghty, H.S. Pereira, F. Grosveld, and M. Antoniou. 1999. Inefficient processing impairs release of RNA from the site of transcription. *EMBO J.* 18:2855–2866.

Dennis, G. Jr., B.T. Sherman, D.A. Hosack, J. Yang, W. Gao, H.C. Lane, and R.A. Lempicki. 2003. DAVID: database for annotation, visualization, and integrated discovery. *Genome Biol.* 4:P3.

Eckner, R., W. Ellmeier, and M.L. Birnstiel. 1991. Mature mRNA 3′ end formation stimulates RNA export from the nucleus. *EMBO J.* 10:3513–3522.

Farny, N.G., J.A. Hurt, and P.A. Silver. 2008. Definition of global and transcript-specific mRNA export pathways in metazoans. *Genes Dev.* 22:66–78.

Fasken, M.B., M. Stewart, and A.H. Corbett. 2008. Functional significance of the interaction between the mRNA-binding protein, Nab2, and the nuclear pore-associated protein, Mlp1, in mRNA export. *J. Biol. Chem.* 283:27130–27143.

Giot, L., J.S. Bader, C. Brouwer, A. Chaudhuri, B. Kuang, Y. Li, Y.L. Hao, C.E. Ooi, B. Godwin, E. Vitols, et al. 2003. A protein interaction map of *Drosophila melanogaster*. *Science.* 302:1727–1736.

Hagiwara, M., and T. Nojima. 2007. Cross-talks between transcription and post-transcriptional events within a 'mRNA factory'. *J. Biochem. (Tokyo).* 142:11–15.

Hall, L.L., K.P. Smith, M. Byron, and J.B. Lawrence. 2006. Molecular anatomy of a speckle. *Anat. Rec. A Discov. Mol. Cell. Evol. Biol.* 288:664–675.

Hammell, C.M., S. Gross, D. Zenklusen, C.V. Heath, F. Stutz, C. Moore, and C.N. Cole. 2002. Coupling of termination, 3′ processing, and mRNA export. *Mol. Cell. Biol.* 22:6441–6457.

Handwerger, K.E., and J.G. Gall. 2006. Subnuclear organelles: new insights into form and function. *Trends Cell Biol.* 16:19–26.

Hector, R.E., K.R. Nykamp, S. Dheur, J.T. Anderson, P.J. Non, C.R. Urbinati, S.M. Wilson, L. Minvielle-Sebastia, and M.S. Swanson. 2002. Dual requirement for yeast hnRNP Nab2p in mRNA poly(A) tail length control and nuclear export. *EMBO J.* 21:1800–1810.

Hilleren, P., and R. Parker. 2001. Defects in the mRNA export factors Rat7p, Gle1p, Mex67p, and Rat8p cause hyperadenylation during 3′-end formation of nascent transcripts. *RNA.* 7:753–764.

Hilleren, P., T. McCarthy, M. Rosbash, R. Parker, and T.H. Jensen. 2001. Quality control of mRNA 3′-end processing is linked to the nuclear exosome. *Nature.* 413:538–542.

Huang, S., T.J. Deerinck, M.H. Ellisman, and D.L. Spector. 1994. In vivo analysis of the stability and transport of nuclear poly(A)+ RNA. *J. Cell Biol.* 126:877–899.

Huang, Y., and G.G. Carmichael. 1996. Role of polyadenylation in nucleocytoplasmic transport of mRNA. *Mol. Cell. Biol.* 16:1534–1542.

Huang, Y., R. Gattoni, J. Stevenin, and J.A. Steitz. 2003. SR splicing factors serve as adapter proteins for TAP-dependent mRNA export. *Mol. Cell.* 11:837–843.

Hutchinson, J.N., A.W. Ensminger, C.M. Clemson, C.R. Lynch, J.B. Lawrence, and A. Chess. 2007. A screen for nuclear transcripts identifies two linked noncoding RNAs associated with SC35 splicing domains. *BMC Genomics.* 8:39.

Ishihama, Y., H. Tadakuma, T. Tani, and T. Funatsu. 2008. The dynamics of pre-mRNAs and poly(A)(+) RNA at speckles in living cells revealed by iFRAP studies. *Exp. Cell Res.* 314:748–762.

Ishizuka, A., M.C. Siomi, and H. Siomi. 2002. A *Drosophila* fragile X protein interacts with components of RNAi and ribosomal proteins. *Genes Dev.* 16:2497–2508.

Jensen, T.H., K. Patricio, T. McCarthy, and M. Rosbash. 2001. A block to mRNA nuclear export in *S. cerevisiae* leads to hyperadenylation of transcripts that accumulate at the site of transcription. *Mol. Cell.* 7:887–898.

Johnson, C., D. Primorac, M. McKinstry, J. McNeil, D. Rowe, and J.B. Lawrence. 2000. Tracking COL1A1 RNA in osteogenesis imperfecta: splice-defective transcripts initiate transport from the gene but are retained within the SC35 domain. *J. Cell Biol.* 150:417–432.

Kerwitz, Y., U. Kuhn, H. Lilie, A. Knoth, T. Scheuermann, H. Friedrich, E. Schwarz, and E. Wahle. 2003. Stimulation of poly(A) polymerase through a direct interaction with the nuclear poly(A) binding protein allosterically regulated by RNA. *EMBO J.* 22:3705–3714.

Kozlova, N., J. Braga, J. Lundgren, J. Rino, P. Young, M. Carmo-Fonseca, and N. Visa. 2006. Studies on the role of NonA in mRNA biogenesis. *Exp. Cell Res.* 312:2619–2630.

Krause, S., S. Fakan, K. Weis, and E. Wahle. 1994. Immunodetection of poly(A) binding protein II in the cell nucleus. *Exp. Cell Res.* 214:75–82.

Lamond, A.I., and D.L. Spector. 2003. Nuclear speckles: a model for nuclear organelles. *Nat. Rev. Mol. Cell Biol.* 4:605–612.

Long, R.M., D.J. Elliott, F. Stutz, M. Rosbash, and R.H. Singer. 1995. Spatial consequences of defective processing of specific yeast mRNAs revealed by fluorescent in situ hybridization. *RNA.* 1:1071–1078.

Luna, R., H. Gaillard, C. Gonzalez-Aguilera, and A. Aguilera. 2008. Biogenesis of mRNPs: integrating different processes in the eukaryotic nucleus. *Chromosoma.* 117:319–331.

Mandel, C.R., Y. Bai, and L. Tong. 2008. Protein factors in pre-mRNA 3′-end processing. *Cell. Mol. Life Sci.* 65:1099–1122.

Masuda, S., R. Das, H. Cheng, E. Hurt, N. Dorman, and R. Reed. 2005. Recruitment of the human TREX complex to mRNA during splicing. *Genes Dev.* 19:1512–1517.

Mintz, P.J., S.D. Patterson, A.F. Neuwald, C.S. Spahr, and D.L. Spector. 1999. Purification and biochemical characterization of interchromatin granule clusters. *EMBO J.* 18:4308–4320.

Molenaar, C., A. Abdulle, A. Gena, H.J. Tanke, and R.W. Dirks. 2004. Poly(A)$^+$ RNAs roam the cell nucleus and pass through speckle domains in transcriptionally active and inactive cells. *J. Cell Biol.* 165:191–202.

Perreault, A., C. Lemieux, and F. Bachand. 2007. Regulation of the nuclear poly(A)-binding protein by arginine methylation in fission yeast. *J. Biol. Chem.* 282:7552–7562.

Politz, J.C., R.A. Tuft, K.V. Prasanth, N. Baudendistel, K.E. Fogarty, L.M. Lifshitz, J. Langowski, D.L. Spector, and T. Pederson. 2006. Rapid, diffusional shuttling of poly(A) RNA between nuclear speckles and the nucleoplasm. *Mol. Biol. Cell.* 17:1239–1249.

Reed, R., and H. Cheng. 2005. TREX, SR proteins and export of mRNA. *Curr. Opin. Cell Biol.* 17:269–273.

Reim, I., J. Mattow, and H. Saumweber. 1999. The RRM protein NonA from *Drosophila* forms a complex with the RRM proteins Hrb87F and S5 and the Zn finger protein PEP on hnRNA. *Exp. Cell Res.* 253:573–586.

Saguez, C., J.R. Olesen, and T.H. Jensen. 2005. Formation of export-competent mRNP: escaping nuclear destruction. *Curr. Opin. Cell Biol.* 17:287–293.

Saitoh, N., C.S. Spahr, S.D. Patterson, P. Bubulya, A.F. Neuwald, and D.L. Spector. 2004. Proteomic analysis of interchromatin granule clusters. *Mol. Biol. Cell.* 15:3876–3890.

Santos-Rosa, H., H. Moreno, G. Simos, A. Segref, B. Fahrenkrog, N. Pante, and E. Hurt. 1998. Nuclear mRNA export requires complex formation between Mex67p and Mtr2p at the nuclear pores. *Mol. Cell. Biol.* 18:6826–6838.

Schmid, M., and T.H. Jensen. 2008. Quality control of mRNP in the nucleus. *Chromosoma.* 117:419–429.

Smith, K.P., P.T. Moen, K.L. Wydner, J.R. Coleman, and J.B. Lawrence. 1999. Processing of endogenous pre-mRNAs in association with SC-35 domains is gene specific. *J. Cell Biol.* 144:617–629.

Smith, K.P., M. Byron, C. Johnson, Y. Xing, and J.B. Lawrence. 2007. Defining early steps in mRNA transport: mutant mRNA in myotonic dystrophy type I is blocked at entry into SC-35 domains. *J. Cell Biol.* 178:951–964.

Sommer, P., and U. Nehrbass. 2005. Quality control of messenger ribonucleoprotein particles in the nucleus and at the pore. *Curr. Opin. Cell Biol.* 17:294–301.

Tavanez, J.P., P. Calado, J. Braga, M. Lafarga, and M. Carmo-Fonseca. 2005. In vivo aggregation properties of the nuclear poly(A)-binding protein PABPN1. *RNA.* 11:752–762.

Veraksa, A., A. Bauer, and S. Artavanis-Tsakonas. 2005. Analyzing protein complexes in *Drosophila* with tandem affinity purification-mass spectrometry. *Dev. Dyn.* 232:827–834.

Wahle, E. 1995. Poly(A) tail length control is caused by termination of processive synthesis. *J. Biol. Chem.* 270:2800–2808.

Windgassen, M., and H. Krebber. 2003. Identification of Gbp2 as a novel poly(A)+ RNA-binding protein involved in the cytoplasmic delivery of messenger RNAs in yeast. *EMBO Rep.* 4:278–283.

Xing, Y., C.V. Johnson, P.T. Moen Jr., J.A. McNeil, and J. Lawrence. 1995. Nonrandom gene organization: structural arrangements of specific pre-mRNA transcription and splicing with SC-35 domains. *J. Cell Biol.* 131:1635–1647.